Copyright © 2008 Tech Science Press CMES, vol.35, no.2, pp.133-154, 2008

Application of Meshless Local Petrov-Galerkin (MLPG) Method in Cloth Simulation

Weiran Yuan[1,2], Yujun Chen[2,3], André Gagalowicz[2] and Kaixin Liu[1]

Abstract: In this paper we present an approach to cloth simulation which models the deformation based on continuum mechanics and discretized with Meshless Local Petrov-Galerkin (MLPG) Method. MLPG method, which involves not only a meshless interpolation for trial functions, but also a meshless integration of the local weak form, has been considered as a general basis for the other meshless methods. By this way, the mechanical behavior of cloth is consistent and united, which is independent of the resolutions. At the same time, point sampled models, which neither have to store nor to maintain globally consistent topological information, are available for MLPG method. We use Kirchhoff-Love (KL) thin shell theory as the basis of the cloth model. Compared to finite element methods, MLPG method provides higher continuity in the displacement field which meets the requirement of the KL model. When large deformation is involved, the nonlinear equations make the simulations become costly. We use corotational formulation to attach the parameterized local coordinate system of nodes. In addition, the rotation fields are computed by an efficient iteration scheme. This allows us to use stable corotated linear strains. As for the collision solution, since the conventional mesh-based collision detection methods fail to work in meshless methods. We developed a novel shape function based collision detection method for the meshless parametric surface. The experimental results show that our cloth simulator based on MLPG method can produce vivid results and can be applied especially in the computer cloth animation.

Keyword: Cloth Simulation, MLPG, Large Deformation, Thin Shells.

[1] LTCS and Department of Mechanics & Aerospace Engineering, College of Engineering, Peking University, Beijing, China

[2] INRIA-Rocquencourt, Paris, France

[3] National Laboratory for Information Science and Technology & Department of Computer Science and Technology, Tsinghua University, Beijing, China

1 Introduction

Physically-based cloth simulation has been widely used in virtual reality, computer animation and textile industry CAD. Till now, mass-spring method is widely used in cloth simulation for its low computational cost and easy implementation [Nealen, Müller, Keiser, Boserman, and Carlson (2005)]. But this method has some natural drawbacks due to the non-continuum configuration, for instance, the material can not be simulated consistently, the results depend on the mesh of springs; the spring parameters lack the basis of physics [Thomaszewski, Wacker, and Straβer (2006)]. While in the textile industry the realistic and authentic cloth behavior is required, one have to resort to the continuum mechanics such as finite element methods [Etzmuβ, Keckeisen, and Straβer (2003)] or meshless methods, to solve the problem. By continuum methods, material behavior can be reproduced accurately, independently of discretization.

Meshless methods have been introduced to computer graphics in recent years and gained increasing attentions as alternative computational methods to the traditional mesh-based methods, such as FEM [Pauly, Keiser, Adams, Dutré, Gross, and Guibas (2005); Guo, Li, Bao, Gu, and Qin (2006); Chang and Zhang (2004)]. Meshless methods have attracted more and more attentions due to their flexibility in solving engineering problems. Among these methods, Meshless Local Petrov-Galerkin method (MLPG) [Atluri and Zhu (1998)] has been considered as a general framework or a general basis for the other meshless methods [Atluri and Shen (2005)]. MLPG involves not only a meshless interpolation for trial functions, but also a meshless integration of the local weak form, i.e., it does not need any background element or mesh. MLPG provides the flexibility in choosing the trial and test functions, as well as the sizes and shapes of local sub-domains, and has been proved to be a truly meshless method [Atluri (2004)]. Therefore MLPG is more flexible and easier to handle the problems from which the conventional Finite Elements (FE) or the other meshless methods suffer.

At the same time, point sampled models, which neither have to store nor to maintain globally consistent topological information, are used in meshless methods. It becomes an ongoing research topic in the field of computer graphics. Although great achievements have been made [Müller, Keiser, Nealen, Pauly, Gross, and Alexa (2004); Guo, Li, Bao, Gu, and Qin (2006)], the full potential of the alternative modeling primitives and the possible areas of application have not yet been fully explored. The application of meshless methods on cloth simulation is an interesting issue.

1.1 Contributions

In this paper, we present a new meshless cloth simulator with Kirchhoff-Love (KL) thin shell theory. The special feathers of cloth as a thin shell bring several problems to traditional meshless methods, for instance, the cloth has different stiffness on the membrane and bending direction. In most of the cloth simulation approaches, the treatments of bending models is done by an angular expression which is not accurate [Thomaszewski, Wacker, and Straβer (2006)]. This means that realistic material parameters and resolution independence can not be expected. However, our method can provide the both the accuracy and the continuum representation. The discretization is based on a MLPG method, which means that the discretization is independent of the geometric subdivision into finite elements. The requirements of consistency are met by the use of a polynomial basis of quadratic or higher order.

When large deformation is involved, the nonlinear equations make the simulations become costly. The finite strain, known as geometrical nonlinearity, is closely linked to the invariance of the measure under rotations. We use corotational formulation to attach the parameterized local coordinate system of nodes. In addition, we compute the rotation field by an efficient iteration scheme. This allows us to use a stable corotated strains.

The collision problem is a difficult problem for the meshless method, since the model does not have the explicit connections and triangles. It makes the traditional collision detection invalid. We propose a detection method based on the moment matrix from shape functions. The shape functions construct the meshless approximation and provide a natural indicator to track the surface. The detection method presented in this paper can detect the contact region by simple criteria.

With the continuum KL thin shell model, the meshless computation, the corotational formulation, the collision detection method, the meshless cloth model can provide realistic and authentic cloth behavior.

1.2 Related Work

In recent years, the meshless methods have been successfully adopted to the computer graphics [Pauly, Keiser, Adams, Dutré, Gross, and Guibas (2005); Chang and Zhang (2004); Guo, Li, Bao, Gu, and Qin (2006)]. Desbrun [Desbrun and Gascuel (1995)] was the first to introduce meshless ideas to the computer graphics area, then the mesh free method was also introduced to the deformable objects. Nealen, Müller, Keiser, Boserman, and Carlson (2005) presented a very nice survey for the deformable objects. Pauly, Keiser, Adams, Dutré, Gross, and Guibas (2005) presented a meshless framework for elastic and plastic materials for fracture. Chang and Zhang (2004) presented the meshless method for animating elastic solids. Guo

and Qin (2005); Guo, Li, Bao, Gu, and Qin (2006) presented a meshless simulation method for volumetric objects and extended to the parametric domain with global parameterization for the thin-shell elastic deformation. Atluri and Zhu (2000) surveyed the up-to-date classification and overview of the meshless methods.

MLPG methods have a bright future to apply in the simulation work of computer graphics. After Atluri's pioneer work [Atluri and Zhu (1998)], it has found a wide range of applications of MLPG methods in analyzing elasto-statics [Atluri and Zhu (2000); Han and Atluri (2004b)], elasto-dynamics [Han and Atluri (2004a)], convection-diffusion problem [Lin and Atluri (2000)], thermoelasticity [Sladek, Sladek, and Atluri (2001); Sladek, Sladek, Zhang, and Tan (2006)], beam problems [Raju and Phillips (2003)], plate problems [Gu and Liu (2001); Long and Atluri (2002); Qian, Batra, and Chen (2003); Sladek, Sladek, Solek, and Wen (2008)], static and dynamic fracture mechanics [Ching and Batra (2001); Gao, Liu, and Liu (2006); Sladek, Sladek, Zhang, Solek, and Starek (2007); Long, Liu, and Li (2008)], thermal analysis [Sladek, Sladek, Zhang, and Solek (2007); Sladek, abd P. Solek, Wen, and Atluri (2008)], magnetic diffusion [Johnson and Owen (2007)], fluid flows [Mohammadi (2008); Arefmanesh, Najafi, and Abdi (2008)]. Vavourakis, Sellountos, and Polyzos (2006) compared the accuracy and stability of five different elasto-static MLPG type formulations. MLPG mixed finite volume method (MFVM) was proposed by Atluri, Han, and Rajendran (2004) to simplify and speed up the meshless implementation for elastostatic problems [Han and Atluri (2004b)], elasto-dynamic problems [Han and Atluri (2004a)], nonlinear problems [Han, Rajendran, and Atluri (2005)], and dynamic problems with large deformation and rotation [Han, Liu, Rajendran, and Atluri (2006); Liu, Han, Rajendran, and Atluri (2006)]. Liu, Han, and Atluri (2006) proposed a MLPG mixed collocation method, which results in a stable convergence rate, while being much more efficient than the MLPG finite volume method. Li and Atluri (2008a) and Li and Atluri (2008b) presented examples of using MLPG mixed collocation method on orthotropic solids and topology-optimization of structures. An MLPG mixed finite difference method was presented by Atluri, Liu, and Han (2006a,b). And Ma (2008) presented a meshless interpolation scheme for MLPG_R Method (Meshless Local Petrove-Galerkin based on Rankine source solution). The three MLPG mixed methods use the mixed approach to interpolate the variables of different orders independently, through the MLS approximation. They demonstrate the flexibility of the MLPG approach, as a general framework, in developing various meshless methods.

Other new meshless methods are also researched on topics of structural dynamic analysis [Liu, Chen, J.Li, and Cen (2008)], quasi-brittle materials [Le, Mai-Duy, Tran-Cong, and Baker (2008)], moving interface problems [Mai-Cao and Tran-

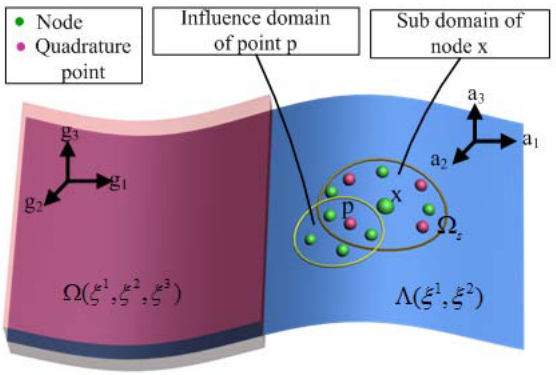

Figure 1: Thin shell model and discretization

Cong (2008)], cracks problems [Rabczuk and Areias (2006), Zhang and Chen (2008), Sageresan and Drathi (2008), Wen, Aliabadi, and Liu (2008)], interior and exterior Dirichlet problems for the two-dimensional Laplace equation [Liu (2007)], fluid-structure-interaction problems [Ahrem, Beckert, and Wendland (2006)] and heat conduction problems [Wu, Shen, and Tao (2007)].

Etzmuβ, Keckeisen, and Straβer (2003) proposed a fast finite element solution for cloth modeling and extracted the rotational part from the displacement field. Thomaszewski, Wacker, and Straβer (2006) presented a method based on a corotational formulation of subdivision finite elements from the simpler 2D problem. They defined $C1$ continuous displacement field.

As for the thin shell method, Grinspun [Grinspun (2004)] presented a discrete shells which can be used to model the aluminum cans and light bulb fracturing. They formulated the dynamics by a discrete model, derived geometrically for triangle meshes. Choi, Woo, and Ko (2007) proposed a real-time simulation technique for thin shell using the energy functions presented by Grinspun. Wicke, Steinemann, and Gross (2005) used the Kirchoff-Love constitutive equations, whose energy captured curvature effects in curved coordinate frames. They combined the thin-shell model with the point model and presented a fibre structure. Sladek, Sladek, Wen, and Aliabadi (2006) applied MLPG methods to solve bending problems of shear deformable shallow shells described by the Reissner theory. Jarak, Soric, and Hoster (2007) analyze shell deformation responses by MLPG methods.

2 Kinematic description

The Kirchhoff-Love (KL) theory assumes the shell to be thin which suits for the cloth. The shell in the 3D space is described in a global cartesian coordinate system $\mathbf{E}^I$. The pair $(\boldsymbol{\varphi}, \mathbf{a}_3)$ defines the position of an arbitrary point of the shell, $\boldsymbol{\varphi}$ gives the position of a point on the shell mid-surface, and $\mathbf{a}_3$ is an unit vector (normal to the shell surface). Figure 1 illustrates the model of KL thin shell theory. The configuration Ω can be put down as

$$\Omega = \left\{ \mathbf{x} \in R^3 | \mathbf{x} = \boldsymbol{\varphi}(\xi^1, \xi^2) + \xi \mathbf{a}_3(\xi^1, \xi^2) \right\}, \tag{1}$$

with $\xi^1, \xi^2 \in \Lambda$ and $\xi \in < h^-, h^+ >$. Here Λ denotes the parametric space, $< h^-, h^+ >$ are the distances of the "lower" and "upper" surfaces of the shell from the reference surface.

We define the convective basis vectors $\mathbf{g}_I$ by the tangent map

$$\begin{aligned} \nabla \mathbf{x}(\xi^1, \xi^2) &= \frac{\partial \mathbf{x}(\xi^1, \xi^2)}{\partial \xi^I} \otimes \mathbf{E}^I = \mathbf{g}_I \otimes \mathbf{E}^I \\ &= \frac{\partial \boldsymbol{\varphi}(\xi^1, \xi^2)}{\partial \xi^I} \otimes \mathbf{E}^I + \xi \frac{\partial \mathbf{a}_3(\xi^1, \xi^2)}{\partial \xi^I} \otimes \mathbf{E}^I, \end{aligned}$$

where the upper Latin subscript I denotes 1 to 3.

In the parametric surface Λ, we define

$$\mathbf{a}_\alpha = \frac{\partial \boldsymbol{\varphi}(\xi^1, \xi^2)}{\partial \xi^\alpha}, \ \mathbf{a}_3 = \frac{\mathbf{a}_1 \times \mathbf{a}_2}{|\mathbf{a}_1 \times \mathbf{a}_2|}, \tag{2}$$

where the Greek indices α range from 1 to 2. The shell director $\mathbf{a}_3$ coincides with the normal to the middle surface of the shell and has the properties:

$$\mathbf{a}_\alpha \cdot \mathbf{a}_3 = 0, \ |\mathbf{a}_3| = 1$$

.

In the configuration Ω, we have the covariant base vectors simply as

$$\begin{aligned} \mathbf{g}_\alpha &= \frac{\partial \mathbf{x}(\xi^1, \xi^2)}{\partial \xi^I} = \mathbf{a}_\alpha + \xi \mathbf{a}_{3,\alpha}, \\ \mathbf{g}_3 &= \frac{\partial \mathbf{x}(\xi^1, \xi^2)}{\partial \xi} = \mathbf{a}_3. \end{aligned} \tag{3}$$

The following contents will use upper-script to denote variables in the reference configuration. For instance $\bar{\varphi}$ is a point on the reference surface; and in the current configuration, variables are without upper-scripts.

The Green-Lagrange strain tensor of the shell is defined as follows,

$$\begin{aligned} E_{IJ} &= \frac{1}{2}(g_{IJ} - \bar{g}_{IJ}) \\ &= \alpha_{IJ} - \xi\beta_{IJ}, \end{aligned} \tag{4}$$

the non-zero components of the tensors α_{IJ} and β_{IJ} are in turn related to the deformation of the shell.

We developed corotational formulation for meshless strain, which will discuss at section 4, so we only need to derive the linearized kinematics. By

$$\mathbf{x}(\xi^1,\xi^2) = \bar{\mathbf{x}}(\xi^1,\xi^2) + \mathbf{u}(\xi^1,\xi^2),$$

where $\mathbf{u}(\xi^1,\xi^2)$ is the displacement field of the middle surface of the shell, we can write the membrance and bending strains as:

$$\alpha_{\alpha\beta} = \frac{1}{2}(\bar{\mathbf{a}}_\alpha \cdot \mathbf{u}_{,\beta} + \mathbf{u}_{,\alpha} \cdot \bar{\mathbf{a}}_\beta), \tag{5}$$

$$\begin{aligned} \beta_{\alpha\beta} &= -\mathbf{u}_{,\alpha\beta} \cdot \bar{\mathbf{a}}_3 \\ &\quad + \frac{1}{|\bar{\mathbf{a}}_1 \times \bar{\mathbf{a}}_2|}[\mathbf{u}_{,1} \cdot (\bar{\mathbf{a}}_{\alpha,\beta} \times \bar{\mathbf{a}}_2) + \mathbf{u}_{,2} \cdot (\bar{\mathbf{a}}_1 \times \bar{\mathbf{a}}_{\alpha,\beta})] \\ &\quad + \frac{\bar{\mathbf{a}}_3 \cdot \bar{\mathbf{a}}_{\alpha,\beta}}{|\bar{\mathbf{a}}_1 \times \bar{\mathbf{a}}_2|}[\mathbf{u}_{,1} \cdot (\bar{\mathbf{a}}_2 \times \bar{\mathbf{a}}_3) + \mathbf{u}_{,2} \cdot (\bar{\mathbf{a}}_3 \times \bar{\mathbf{a}}_1)]. \end{aligned} \tag{6}$$

We can conclude from these expressions that the displacement field **u** of the middle surface furnishes a complete description of the deformation of the shell. So we regard **u** as the primary unknown of the analysis. It follows from these relations that, by virtue of the assumed Kirchhoff-Love kinematics, all the strain measures of interest may be deduced from the deformation of the middle surface of the shell.

3 Meshless numerical discretization

3.1 Interpolation approximation

For a so-called meshless implementation, a meshless interpolation scheme is required, in order to approximate the trial function over the solution domain. Actually, meshless methods can be classified according to the meshless approximation method used.

In our work, the augmented radial basis functions (RBF) approximations are used to construct shape functions. They have some distinct advantages over the widely used moving least squares(MLS) approximation, including the shape functions possess

the delta function property and the second derivatives of the shape function are smoother, and are computationally less costly. Its delta function property makes it possible to directly enforce the essential boundary conditions.

Figure 1 illustrates the KL thin shell representation and the meshless sub-domains. Consider a sub-domain Ω_s of a point $\mathbf{x}$, which is local in the solution domain. To approximate the distribution of function u in Ω_s, over a number of scatterd points $\{\mathbf{x}_i\}, (i = 1,2,...,n)$,the local augmented interpolation of both RBF and MLS can be expressed as standard form

$$u(\mathbf{x}) = \mathbf{\Phi}^T(\mathbf{x})\mathbf{u}, \ \forall \mathbf{x} \in \Omega_s, \tag{7}$$

with $\Phi(\mathbf{x})$ being the shape functions. We take RBF interpolation for example:

$$\mathbf{\Phi}^T(\mathbf{x}) = \left[\mathbf{R}^T(\mathbf{x}), \mathbf{P}^T(\mathbf{x})\right]\mathbf{G}, \tag{8}$$

where $\mathbf{R}^T(\mathbf{x}) = [R_1(\mathbf{x}), R_2(\mathbf{x}), ..., R_n(\mathbf{x})]$ is a set of radial basis functions centered around the n scattered points, $\mathbf{P}^T(\mathbf{x}) = [p_1(\mathbf{x}), p_2(\mathbf{x}), ..., p_m(\mathbf{x})]$ is a monomial basis of order m. $\mathbf{G}$ is a matrix composited by R and P at the scattered points:

$$\begin{aligned} \mathbf{G} &= \begin{bmatrix} \mathbf{R}_0 & \mathbf{P}_0 \\ \mathbf{P}_0^T & 0 \end{bmatrix}^{-1}, \\ \mathbf{R}_0 &= \left[\mathbf{R}^T(\mathbf{x}_i)\right], \mathbf{P}_0 = \left[\mathbf{P}^T(\mathbf{x}_i)\right], \ i = 1,2,...,n \end{aligned}$$

The derivatives of $u(\mathbf{x})$ can be simply expressed using the derivatives of the shape function $\Phi_I(\mathbf{x})$,

$$u_{,j}(\mathbf{x}) = \left\{\Phi_{I,j}(\mathbf{x})\right\}^T \{u_I\}. \tag{9}$$

As at least C^1 continuity is required for shape functions $\Phi_I(\mathbf{x})$ in shells, special techniques must be adopted to model surfaces with discontinuities in geometry such as crease, such surfaces might have to be split with appropriate boundary conditions imposed at the seam line.

3.2 Surface and displacement approximation

In point based graphics, object as cloth can be rendered only use the coordinates of scattered points on surface. The present approach is targeted at cloth as general shells. It means that we have to deal with the issue of surface shape approximation. Naturally, the method of computing shape function can be applied to fit the approximate surface to a collection of scattered data points.

The RBF or MLS technique can be applied immediately to obtain the surface approximation. Let us assume that a set of m scattered points in space is given. These

points lie directly on the surface to be approximated at locations $\mathbf{x_I}$. The approximate surface and displacement then may be described by

$$\boldsymbol{\varphi}(\xi^1,\xi^2) = \sum_{I=1}^{m} \Phi_I(\xi^{\mathbf{1}},\xi^{\mathbf{2}})\mathbf{x_I}, \tag{10}$$

$$\mathbf{u}(\xi^1,\xi^2) = \sum_{I=1}^{m} \Phi_I(\xi^{\mathbf{1}},\xi^{\mathbf{2}})\mathbf{u}_I. \tag{11}$$

where ξ^1,ξ^2 is the parameterization of the surface. Note that to evaluate the derivatives of the displacement vector $\mathbf{u}(\xi^{\mathbf{1}},\xi^{\mathbf{2}})$ one needs only to differentiate the shape function $\Phi_I(\xi^1,\xi^2)$. This means that the smoothness of the displacement approximation depends on the smoothness of the shape function. To compute the strains one needs only second order derivatives with respect to the parameters ξ^1,ξ^2.

3.3 Dynamics system equations

We can relate a pair of energy conjugated strain and stress E and S with a material law as

$$S = C(E)$$

In stable elastic equilibrium situations the total energy must be at a minimum. Mathematically, the weak form of the equilibrium equation can be formulated by setting the first varitation of energy to zero

$$\int_\Omega \delta E : S d\Omega - \int_\Omega \delta\mathbf{u}\cdot\mathbf{q}d\Omega + \int_\Omega \nu\delta\mathbf{u}\cdot\dot{\mathbf{u}}d\Omega + \int_\Omega \rho\delta\mathbf{u}\cdot\ddot{\mathbf{u}}d\Omega \qquad = 0 \tag{12}$$

where the three terms account for elastic strain energy, potential energy due to applied force, viscosity force and inertial force. With the definition of the membrane and bending strains and stress, the elastic strain energy can be rewritten as

$$\int_\Omega \delta E : S d\Omega = \int_\Omega (\delta\alpha^T\mathbf{H}_m\alpha + \delta\beta^T\mathbf{H}_b\beta)d\Omega, \tag{13}$$

where $\mathbf{H}_m$ and $\mathbf{H}_b$ are matrices corresponding to the membrane and bending part of the material law, which are the same with the FEM, refer to Cirak, Ortiz, and Schroder (2000) for more details of $\mathbf{H}$.

Owning to the linear relationship between α,β and $\mathbf{u}$ from equation (5) to (6), and the approximation of displacement $\mathbf{u}$ by the nodal displacement $\mathbf{u}_I$ in equation (7), we obtain:

$$\alpha(\xi^1,\xi^2) = \sum_{I=1}^{m} \mathbf{R}_m^I(\xi^1,\xi^2)\mathbf{u}_I, \tag{14}$$

$$\beta(\xi^1,\xi^2)=\sum_{I=1}^{m}\mathbf{R}_b^I(\xi^1,\xi^2)\mathbf{u}_I, \tag{15}$$

where $\mathbf{R}_m^I$ and $\mathbf{R}_\mathbf{b}^\mathbf{I}$ are matrices relating nodal displacement to membrane and bending strain.

The dynamics equation in form of the second order ordinary differential equation in time is

$$\mathbf{M}\ddot{\mathbf{u}}+\mathbf{D}\dot{\mathbf{u}}+\mathbf{K}\mathbf{u}=\mathbf{f}, \tag{16}$$

where $\mathbf{M}$ is the diagonal nodal mass matrix, $\mathbf{D}$ is the viscosity matrix and $\mathbf{K}$ is the stiffness matrix, with the nodal displacement vector $\mathbf{u}$ and forces vector $\mathbf{f}$.

In MLPG approaches, one may write a weak form over a local sub-domain Ω_s of a point $\mathbf{x}_k$, which may have an arbitrary shape. Application equation (12) to (15) , a generalized local weak form corresponding to the stiffness matrix and nodal force vector of equation (16) will be

$$\mathbf{K}_k^{IJ}=\int_{\Omega_s}\left[(\mathbf{R}_m^I)^T\mathbf{H}_m\mathbf{R}_m^J+(\mathbf{R}_b^I)^T\mathbf{H}_b\mathbf{R}_b^J\right]d\Omega, \tag{17}$$

$$\mathbf{f}_k^I=\int_{\Omega_s}\Phi_I\mathbf{q}d\Omega. \tag{18}$$

The stiffness matrix is evaluated by numerical integration in the local domain Ω_s. Usually, Gaussian integration will be applied. Owe to the arbitrary shape of the local domain, it does not need any mesh or background mesh for the integration of the weak forms.

For numerical solution, equation (16) is translated into the first order ODEs and any time integration scheme can be applied. The arising linear system of equations with nodal velocities as primary unknowns is a large and usually sparse system, which can be solved by direct factorization methods [Yuan, Chen, and Liu (2007)] or iteration factorization methods.

4 Meshless corotational formulation for large deformation

Green-Lagrange strain tensor leads to a nonlinear ODE. The corotational formulation aims at the elimination of the geometrical nonlinearity. The idea is to keep track of a rotated local coordinate system of every nodes of the body.

We linearized the strain in equation 5 and 6, so the strain in the former kinematic description is linear in displacement but not rotationally invariant anymore. However, if the rotation field R is known, the corotational strain formulation can be used and we obtain the rotated linear strain tensor on the rotated current configuration.

With equation (1) and (2), the deformation gradient can be written as

$$F = \frac{\partial \mathbf{x}}{\partial \bar{\mathbf{x}}} = \frac{\partial \mathbf{x}}{\partial \xi^I} \otimes \bar{\mathbf{g}}^I = [\mathbf{a}_\alpha + \xi \mathbf{a}_{3,\alpha}] \otimes \bar{\mathbf{g}}^\alpha + \mathbf{a}_3 \otimes \bar{\mathbf{g}}^3 \tag{19}$$

Via polar decomposition the deformation gradient tensor F can be split into a rotational tensor R and a pure deformation U as

$$F = RU$$

Higham and Schreiber (1990) proposed an efficient, quadratically convergent iteration scheme to extract rotation field from deformation gradient

$$R^0 := F \tag{20}$$

$$R^{n+1} := \frac{1}{2}\left(R^n + (R^n)^{-T}\right). \tag{21}$$

This abtains a very fast and accuracy controlled method of computing R. The iteration is defined for square, nonsingular matrices only, but Higham also present a preliminary QR decomposition enables the treatment of singular matrix.

With the rotated field $\mathbf{R}$, the stiffness matrix $\mathbf{Ku}$ becomes $\mathbf{RKu}^R$. In the nodal view of node I , the displacement influence nodes J is $u_J^R = R_I^T(\bar{x}_J + u_J - x_I) + (x_I - \bar{x}_J)$. Therefore, the dynamics system equation (16) can be rewritten as

$$\mathbf{M\ddot{u}} + \mathbf{D\dot{u}} + \mathbf{RKR}^T\mathbf{u} = \mathbf{f} + \mathbf{RK}(\mathbf{R}^T - \mathbf{I})(\mathbf{x}_{node} - \mathbf{x}). \tag{22}$$

Now the system to be solved in each time step remain linear. Compared to classical linear meshless methods, the linear system change over time, whenever the reference configurations are updated.

5 Collision detection of Meshless surface

For the collision detection, as the meshless methods don't maintain the mesh of the surface, therefore the conventional mesh-based collision detection methods, e.g. vertex-to-face and face-to-face detection, fail to work. We present a new collision detection method based on the shape function for the meshless point surface . It aims to decide whether a node is in collision with the other parts of the meshless cloth surface. Take the node positioned at P as example, in the next timestep the position will be Q. If P will have a collision with the cloth, then PQ will intersect with the parametric surface in this time step. We assume the intersection point as M.

Then the problem can be separated into two steps. At first we determine whether the intersection point M exists and compute the parametric coordinates of M; Secondly, on the parametric surface, determine whether M is inside the domain of cloth. It's quite easy to get M via project P to the surface (note the projection point as P') and express the parametric coordinates of M by the parametric coordinates of P'. Then the second step is simplified to a collision problem of meshless domain in two dimensional space.

In our meshless interpolation methods, the construction of shape function (equation 8) requires computing of matrix

$$\mathbf{N} = \begin{bmatrix} \mathbf{R}_0 & \mathbf{P}_0 \\ \mathbf{P}_0^T & 0 \end{bmatrix}. \tag{23}$$

It has been found that this matrix provides a natrual indicator to track the surface of the continuum object. Based on the matrix $\mathbf{N}$ from shape function, the collision detection in two dimensional parametric space can be done simply and accurately. Li, Qian, Liu, and Belytschko (2001) proved that the internal position of a continuum domain and the external can be distinguished by checking the determinant of the matrix $\mathbf{N}$. Inside the continuum domain of any shape, $det\{\mathbf{N}(x)\}$ has a positive value, and outside the domain $det\{\mathbf{N}(x)\} \to 0$. The usefulness of above property is that one can accurately track the position of any continuum without knowing the exact shape of its boundary, which is almost impossible to know in general meshless models. Therefore we can track if the intersection point M is in the internal cloth domain or in the external (or holes on cloth).

The collision response is available through different approaches. Physically, it can be done by adding a penalty force or constraints between the contacting nodes. All these response methods are same as the mesh-based methods. The $\mathbf{a}_3$ of the intersection point M (choose between $\mathbf{a}_3$ and $-\mathbf{a}_3$ according to the position of P) can be used as an indication of the direction to eliminate collision and $\tau = \frac{|PQ|}{|PM|}$, the ratio of crossed part of PQ, as an indication of the amount of penalty force or position of constraints.

6 Implementation

The implementation of the numerical part of the proposed method can be carried out according to the following outline in Figure 3.

Because the shape functions are computed from the parametric surface Λ, storage of the computed $\mathbf{R}(\mathbf{x})$ and $\mathbf{P}(\mathbf{x})$ for computing points and $\mathbf{G}$ for nodes may accelerates the whole procedure. The neighbor nodes in a subdomain Ω_s of a computing point $\mathbf{x}$ can also be searched for only one times. These are all benefit from the constant coordinates in the parametric surface Λ.

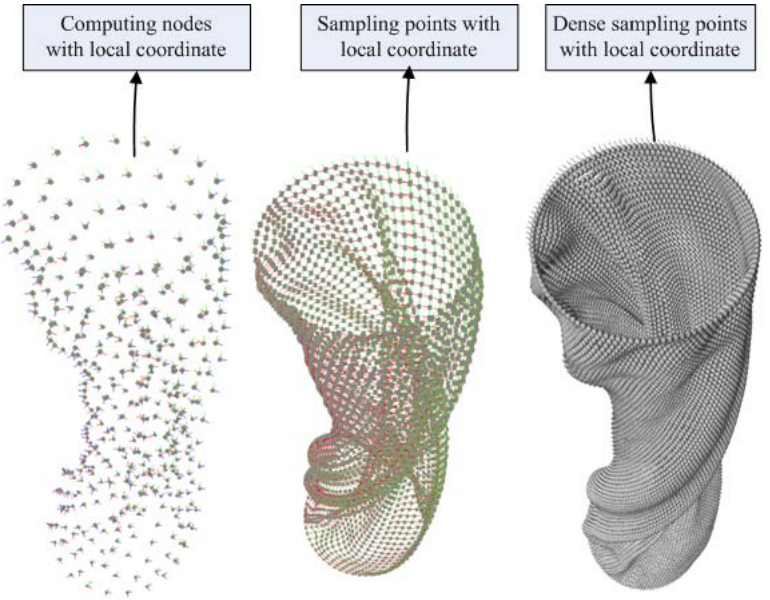

Figure 2: Computing nodes and sampling points

For the matiral parameters, we use the same idea with Thomaszewski, Wacker, and Straβer (2006) and take the Kawabata measurements [Kawabata (1980)] of real fabric samples, which makes the parameter more realistic. Kawabata measurements are standard equipments that can measure the cloth behaviour in weft and warf directions. They can reflect the textile parameters that controls the bending and draping. The elastic parameters can be obtained from Kawabata measurements and be assumed a purely elastic stress. The poisson coeficient cannot be estimated from Kawabata experiments and we set a values about 0.3 which are close to the Poisson numbers used by Thomaszewski, Wacker, and Straβer (2006). For the viscous material parameters, we choose a constant fraction of the corresponding elastic parameter. We used implicit time integration [Baraff and Witkin (1998)] and this implicit method has already been applied in our another cloth simulator emillion which is based on the mass spring model [Gagalowicz (2006)].

7 Results

In this section we present our experimental results on our meshless cloth simulator. The elasticity coefficient (Young's modulus) E= 10000N/m and Poisson's ratio $\nu =$ 0.3. Through the experimental results we can see that the meshless method can treat the cloth with large deformation.

Figure 3: Implementation outline

1. Parameterize the given cloth model Ω to the mid-surface Λ. Determine the undeformed configuration and the beginning configuration.
2. Choose a finite number of nodes on the parametrized mid-surface Λ.
3. Determine the local sub-domain Ω_s for each node.
4. Compute G of each node; compute the shape functions Φ_I in the definition domain of each node; and compute the derivatives of node coordinates.
5. Loop over all nodes located inside the global domain
   (a) Determine Gaussian quadrature points $\mathbf{x}_Q$ in the subdomain Ω_s.
   (b) Loop over quadrature points $\mathbf{x}_Q$
      i. calculate the shape function and the derivatives;
      ii. evaluate numerical integrals;
      iii. assemble contributions to the system equation for all nodes in $\mathbf{K}$.
6. End node loop.
7. Assemble $\mathbf{M}$, $\mathbf{D}$ for the dynamics equations.
8. Loop over all time steps, the interval is δt
   - Compute rotated $\mathbf{K}$;
   - Filter $\mathbf{K}$, $\mathbf{M}$ and $\mathbf{D}$ if using constraints.
   - Composite the linear system depending on the type of time integration;
   - Solve the arising linear system and obtain the velocity $\dot{\mathbf{u}}$;
   - Update the unknown variables and their derivatives at the sample points;
   - Collision detection;
   - Extract the new rotation field;
   - Resample if needs to generate a rendering frame.
9. End time step loop.

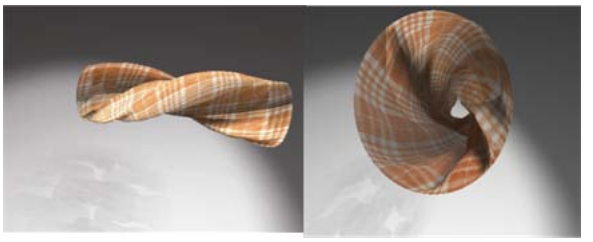

Figure 4: Results of the cylindrical sleeves with the twisting force

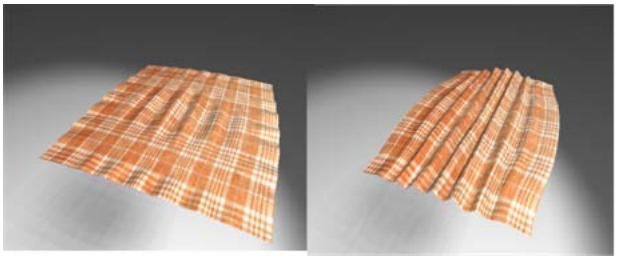

Figure 5: Results of buckling effects

Figure 6: Results of a cloth dropping on a truncheon

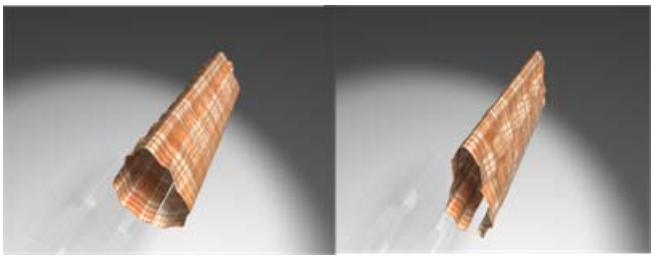

Figure 7: Results of a cylindrical cloth draping on its middle line

The first example, We simulate the cylindrical sleeves with the twisting force. The cylindrical sleeves are the most frequently used examples in the cloth simulation research and can well judge the validity for buckling and folds for the simulator. The cylindrical sleeves are also the basic elements of the virtual garment and it can prove the potential capability for the virtual dressing. In this example, only 20×20 nodes are modeled for the simulation. The time for computing the deformation is nearly realtime for the small amount of nodes. The reason for the low computation is that the most time consuming parts of the simulator is at the assembling the stiffness matrix. Figure 2 shows the original computational nodes with the local coordinates drawn in each nodes, and the thicker sampling points for the rendering. After obtaining the stiffness matrix, in each time step there is no time consuming computation. At the same time, it can obtain accurate results to any precision as it uses the continuum formulation with the RBF function. In figure 4, the folds are clearly reproduced and the process of the twisting act the similar behaviors as observed with the real fabrics. The realistic shapes of the meshless cloth simulation results are undoubtedly because of we use the continuum and consistent way to model the cloth and the sampling and rending of the meshless surface can take advantage of the research achievements from the point based graphics.

This approach can also produce the buckling effects which is also one of the most complicated problems in cloth simulation. In figure 5, the flat cloth undergoes the boundary force. In the system without buckling treating, it will result to a instability status. From the example, the small bucks and folds are produced. Another experiment is the cloth dropping on a truncheon. Figure 6 shows the dynamic procedure of the results. Figure 7 shows a cylindrical cloth without sewing draping on its middle line. The examples below show the small buckles and wrinkles produced by the simulator. These experiments testify the cloth simulator.

8 Conclusion and Future work

We have shown that the MLPG method with KL theory can be used for modeling cloth more accurately. A novel achievement of the presented work is the combination of this new approach with corotational formulation resulting a linear system, which leads to an efficient implementation. We also present the collision detection method for the meshless simulator. The computation of meshless method mainly comes from the numerical integration, smaller number of quadratic points will speed up the simulation but reduce the precision. Now there is sufficient computational power available, which allows to use physically accurate modeling on nearly real-time simulations.

The future work may include integration of the garment design system as the preprocess of the simulator in order to get the results of composite model of the gar-

ment. The application of the meshless cloth simulator is appealing.

Acknowledgement: The authors gratefully acknowledge the financial support of the National Natural Science Foundation of China (grant nos.: 10572002, 10732010)

References

Ahrem, R.; Beckert, A.; Wendland, H. (2006): A meshless spatial coupling scheme for large-scale fluid-structure-interaction problems. *CMES-COMPUTER MODELING IN ENGINEERING & SCIENCES*, vol. 12, pp. 121–136.

Arefmanesh, A.; Najafi, M.; Abdi, H. (2008): Meshless local Petrov-Galerkin method with unity test function for non-isothermal fluid flow. *CMES-COMPUTER MODELING IN ENGINEERING & SCIENCES*, vol. 25, no. 1, pp. 9–22.

Atluri, S. N. (2004): *The Meshless Local Petrov-Galerkin (MLPG) Method for Domain & Boundary Discretizations*. Tech Science Press, Los Angeles, CA.

Atluri, S. N.; Han, Z. D.; Rajendran, A. M. (2004): A new implementation of the meshless finite volume method through the MLPG "mixed" approach. *CMES-COMPUTER MODELING IN ENGINEERING & SCIENCES*, vol. 6, no. 6, pp. 491–513.

Atluri, S. N.; Liu, H. T.; Han, Z. D. (2006): Meshless local Petrov-Galerkin (MLPG) mixed collocation method for elasticity problems. *CMES-COMPUTER MODELING IN ENGINEERING & SCIENCES*, vol. 14, no. 3, pp. 141–152.

Atluri, S. N.; Liu, H. T.; Han, Z. D. (2006): Meshless local Petrov-Galerkin (MLPG) mixed finite difference method for solid mechanics. *CMES-COMPUTER MODELING IN ENGINEERING & SCIENCES*, vol. 15, no. 1, pp. 1–16.

Atluri, S. N.; Shen, S. (2005): The basis of meshless domain discretization: the meshless local Petrov-Galerkin (MLPG) method. *Advances in Computational Mathematics*, vol. 23, pp. 79–93.

Atluri, S. N.; Zhu, T. (1998): A new meshless local Petrov-Galerkin (MLPG) approach in computational mechanics. *Comput. Mech. J.*, vol. 22, pp. 117–127.

Atluri, S. N.; Zhu, T. (2000): The meshless local Petrov-Galerkin (MLPG) approach for solving problems in elasto-statics. *Comput. Mech. J.*, vol. 25, pp. 169–179.

Baraff, D.; Witkin, A. (1998): Large steps in cloth simulation. In *SIGGRAPH '98: Proceedings of the 25th annual conference on Computer graphics and interactive techniques*, pp. 43–54, New York, NY, USA. ACM.

Chang, J.; Zhang, J. (2004): Mesh-free deformations. *Computer Animation and Virtual Worlds*, vol. 15, no. 3-4, pp. 211–218.

Ching, H. K.; Batra, R. C. (2001): Determination of crack tip fields in linear elastostatics by the meshless local Petrov-Galerkin (MLPG) method. *CMES-COMPUTER MODELING IN ENGINEERING & SCIENCES*, vol. 2, no. 2, pp. 273–289.

Choi, M. G.; Woo, S. Y.; Ko, H.-S. (2007): Real-time simulation of thin shells. *Computer Graphics Forum*, vol. 26, pp. 349–354.

Cirak, F.; Ortiz, M.; Schroder, P. (2000): Subdivision surfaces: a new paradigm for thin-shell finite-element analysis. *International Journal for Numerical Methods in Engineering*, vol. 47, no. 12, pp. 2039–2072.

Desbrun, M.; Gascuel, M.-P. (1995): Animating soft substances with implicit surfaces. In *SIGGRAPH '95: Proceedings of the 22nd annual conference on Computer graphics and interactive techniques*, pp. 287–290, New York, NY, USA. ACM.

Etzmuβ, O.; Keckeisen, M.; Straβer, W. (2003): A fast finite element solution for cloth modelling. In *PG '03: Proceedings of the 11th Pacific Conference on Computer Graphics and Applications*, pg. 244, Washington, DC, USA. IEEE Computer Society.

Gagalowicz, A. (2006): Object manipulation in image sequences for augmented reality and special effects, 2006 research project activity report. Technical report, INRIA,Rocquencourt, 2006.

Gao, L.; Liu, K.; Liu, Y. (2006): Applications of MLPG method in dynamic fracture problems. *CMES-COMPUTER MODELING IN ENGINEERING & SCIENCES*, vol. 181–195, no. 3, pp. 12.

Grinspun, E. (2004): A discrete model for inelastic deformation of thin shells. In *In ACM/Eurographics Symposium on Computer Animation*.

Gu, Y. T.; Liu, G. R. (2001): A meshless local Petrov-Galerkin (MLPG) formulation for static and free vibration analysis of thin plate. *CMES-COMPUTER MODELING IN ENGINEERING & SCIENCES*, vol. 2, no. 4, pp. 463–476.

Guo, X.; Li, X.; Bao, Y.; Gu, X.; Qin, H. (2006): Meshless thin-shell simulation based on global conformal parameterization. *IEEE Trans Vis Comput Graph*, vol. 12, no. 3, pp. 375–385.

Guo, X. H.; Qin, H. (2005): Real-time meshless deformation. *Computer Animation and Virtual Worlds*, vol. 16, pp. 189–200.

Han, Z. D.; Atluri, S. N. (2004): Meshless local Petrov-Galerkin (MLPG) approach for 3-dimensional elasto-dynamics. *Comput, Mater. Continua*, vol. 1, no. 2, pp. 129–140.

Han, Z. D.; Atluri, S. N. (2004): Meshless local Petrov-Galerkin (MLPG) approache for solving 3d problem in elasto statics. *Comp.Model Engr*, vol. 6, no. 2, pp. 169–188.

Han, Z. D.; Liu, H. T.; Rajendran, A. M.; Atluri, S. N. (2006): The applications of meshless local Petrov-Galerkin (MLPG) approaches in high-speed impact, penetration and perforation problems. *CMES-COMPUTER MODELING IN ENGINEERING & SCIENCES*, vol. 14, no. 2, pp. 119–128.

Han, Z. D.; Rajendran, A. M.; Atluri, S. N. (2005): Meshless local Petrov-Galerkin (MLPG) approaches for solving nonlinear problems with large deformations and rotations. *CMES-COMPUTER MODELING IN ENGINEERING & SCIENCES*, vol. 10, no. 1, pp. 1–12.

Higham, N. J.; Schreiber, R. S. (1990): Fast polar decomposition of an arbitrary matrix. *SIAM Journal on Scientific and Statistical Computing*, vol. 11, no. 4, pp. 648–655.

Jarak, T.; Soric, J.; Hoster, J. (2007): Analysis of shell deformation responses by the meshless local Petrov-Galerkin (MLPG) approach. *CMES-COMPUTER MODELING IN ENGINEERING & SCIENCES*, vol. 18, no. 3, pp. 235–246.

Johnson, J.; Owen, J. (2007): A meshless local Petrov-Galerkin method for magnetic diffusion in non-magnetic conductors. *CMES-COMPUTER MODELING IN ENGINEERING & SCIENCES*, vol. 22, no. 3, pp. 165–188.

Kawabata, S. (1980): *The Standardization and Analysis of Hand Evaluation*. 1980Osaka: Textile Machinery Society of Japan.

Le, P.; Mai-Duy, N.; Tran-Cong, T.; Baker, G. (2008): A meshless modeling of dynamic strain localization in quasi-brittle materials using radial basis function networks. *CMES-COMPUTER MODELING IN ENGINEERING & SCIENCES*, vol. 25, pp. 43–66.

Li, S.; Atluri, S. N. (2008): The MLPG mixed collocation method for material orientation and topology optimization of anisotropic solids and structures. *CMES-COMPUTER MODELING IN ENGINEERING & SCIENCES*, vol. 30, no. 1, pp. 37–56.

Li, S.; Atluri, S. N. (2008): Topology-optimization of structures based on the mlpg mixed collocation method. *CMES-COMPUTER MODELING IN ENGINEERING & SCIENCES*, vol. 26, no. 1, pp. 61–74.

Li, S.; Qian, D.; Liu, W. K.; Belytschko, T. (2001): A meshfree contact-detection algorithm. *Computer Methods in Applied Mechanics and Engineering*, vol. 190, pp. 3271–3292.

Lin, H.; Atluri, S. N. (2000): Meshless local Petrov-Galerkin (MLPG) method for convection-diffusion problems. *CMES-COMPUTER MODELING IN ENGINEERING & SCIENCES*, vol. 1, no. 2, pp. 45–60.

Liu, C.-S. (2007): A meshless regularized integral equation method for laplace equation in arbitrary interior or exterior plane domains. *CMES-COMPUTER MODELING IN ENGINEERING & SCIENCES*, vol. 19, pp. 99–109.

Liu, H. T.; Han, Z. D.; Atluri, S. N. (2006): Meshless local Petrov-Galerkin (MLPG) mixed collocation method for elasticity problems. *CMES-COMPUTER MODELING IN ENGINEERING & SCIENCES*, vol. 14, no. 3, pp. 141–152.

Liu, H. T.; Han, Z. D.; Rajendran, A. M.; Atluri, S. N. (2006): Computational modeling of impact response with the rg damage model and the meshless local Petrov-Galerkin (MLPG) approaches. *CMC: Computers, Materials & Continua*, vol. 4, no. 1, pp. 43–54.

Liu, Y. H.; Chen, S. S.; J.Li; Cen, Z. Z. (2008): A meshless local natural neighbour interpolation method applied to structural dynamic analysis. *CMES-COMPUTER MODELING IN ENGINEERING & SCIENCES*, vol. 31, pp. 145–156.

Long, S.; Liu, K.; Li, G. (2008): An analysis for the elasto-plastic fracture problem by the meshless local Petrov-Galerkin method. *CMES-COMPUTER MODELING IN ENGINEERING & SCIENCES*, vol. 28, no. 3, pp. 203–216.

Long, S. Y.; Atluri, S. N. (2002): A meshless local Petrov-Galerkin method for solving the beding problem of a thin plate. *CMES-COMPUTER MODELING IN ENGINEERING & SCIENCES*, vol. 3, no. 1, pp. 53–63.

Ma, Q. (2008): A new meshless interpolation scheme for mlpg_r method. *CMES-COMPUTER MODELING IN ENGINEERING & SCIENCES*, vol. 23, pp. 75–89.

Mai-Cao, L.; Tran-Cong, T. (2008): A meshless approach to capturing moving interfaces in passive transport problems. *CMES-COMPUTER MODELING IN ENGINEERING & SCIENCES*, vol. 31, pp. 157–188.

Mohammadi, M. H. (2008): Stabilized meshless local Petrov-Galerkin (MLPG) method for incompressible viscous fluid flows. *CMES-COMPUTER MODELING IN ENGINEERING & SCIENCES*, vol. 29, no. 2, pp. 75–94.

Müller, M.; Keiser, R.; Nealen, A.; Pauly, M.; Gross, M.; Alexa, M. (2004): Point based animation of elastic, plastic and melting objects. In *SCA '04: Proceedings of the 2004 ACM SIGGRAPH/Eurographics symposium on Computer animation*, pp. 141–151, Aire-la-Ville, Switzerland, Switzerland. Eurographics Association.

Nealen, A.; Müller, M.; Keiser, R.; Boserman, E.; Carlson, M. (2005): Physically based deformable models in computer graphics. *Computer Graphics Forum*, vol. 25, no. 4, pp. 809–836.

Pauly, M.; Keiser, R.; Adams, B.; Dutré, P.; Gross, M.; Guibas, L. J. (2005): Meshless animation of fracturing solids. *ACM Trans. Graph.*, vol. 24, no. 3, pp. 957–964.

Qian, L. F.; Batra, R. C.; Chen, L. M. (2003): Elastostatic deformations of a thick plate by using a higherorder shear and normal deformable plate theory and two meshless local Petrov-Galerkin (MLPG) methods. *CMES-COMPUTER MODELING IN ENGINEERING & SCIENCES*, vol. 4, no. 1, pp. 161–176.

Rabczuk, T.; Areias, P. (2006): A meshfree thin shell for arbitrary evolving cracks based on an extrinsic basis. *CMES-COMPUTER MODELING IN ENGINEERING & SCIENCES*, vol. 16, pp. 115–130.

Raju, I. S.; Phillips, D. R. (2003): Further developments in the MLPG method for beam problems. *CMES-COMPUTER MODELING IN ENGINEERING & SCIENCES*, vol. 4, no. 1, pp. 141–160.

Sageresan, N.; Drathi, R. (2008): Crack propagation in concrete using meshless method. *CMES-COMPUTER MODELING IN ENGINEERING & SCIENCES*, vol. 32, pp. 103–112.

Sladek, J.; abd P. Solek, V. S.; Wen, P.; Atluri, S. (2008): Thermal analysis of reissner-mindlin shallow shells with FGM properties by the MLPG. *CMES-COMPUTER MODELING IN ENGINEERING & SCIENCES*, vol. 30, no. 2, pp. 77–98.

Sladek, J.; Sladek, V.; Atluri, S. N. (2001): A pure contour formulation for the meshless local boundary integral equation method in thermoelasticity. *CMES-COMPUTER MODELING IN ENGINEERING & SCIENCES*, vol. 2, no. 4, pp. 423–434.

Sladek, J.; Sladek, V.; Solek, P.; Wen, P. (2008): Thermal bending of reissner-mindlin plates by the MLPG. *CMES-COMPUTER MODELING IN ENGINEERING & SCIENCES*, vol. 28, no. 1, pp. 57–67.

Sladek, J.; Sladek, V.; Wen, P. H.; Aliabadi, M. (2006): Meshless local Petrov-Galerkin (MLPG) method for shear deformable shells analysis. *CMES-COMPUTER MODELING IN ENGINEERING & SCIENCES*, vol. 13, no. 2, pp. 103–117.

Sladek, J.; Sladek, V.; Zhang, C.; Solek, P. (2007): Application of the mlpg to thermo-piezoelectricity. *CMES-COMPUTER MODELING IN ENGINEERING & SCIENCES*, vol. 22, no. 3, pp. 217–234.

Sladek, J.; Sladek, V.; Zhang, C.; Solek, P.; Starek, L. (2007): Fracture analyses in continuously nonhomogeneous piezoelectric solids by the mlpg. *CMES-COMPUTER MODELING IN ENGINEERING & SCIENCES*, vol. 19, no. 3, pp. 247–262.

Sladek, J.; Sladek, V.; Zhang, C.; Tan, C. L. (2006): Meshless local Petrov-Galerkin method for linear coupled thermoelastic analysis. *CMES-COMPUTER MODELING IN ENGINEERING & SCIENCES*, vol. 16, no. 1, pp. 57–68.

Thomaszewski, B.; Wacker, M.; Straβer, W. (2006): A consistent bending model for cloth simulation with corotational subdivision finite elements. In *SCA '06: Proceedings of the 2006 ACM SIGGRAPH/Eurographics symposium on Computer animation*, pp. 107–116, Aire-la-Ville, Switzerland, Switzerland. Eurographics Association.

Vavourakis, V.; Sellountos, E. J.; Polyzos, D. (2006): A comparison study on different MLPG(lbie) formulations. *CMES-COMPUTER MODELING IN ENGINEERING & SCIENCES*, vol. 13, no. 3, pp. 171–184.

Wen, P.; Aliabadi, M.; Liu, Y. (2008): Meshless method for crack analysis in functionally graded materials with enriched radial base functions. *CMES-COMPUTER MODELING IN ENGINEERING & SCIENCES*, vol. 30, pp. 133–147.

Wicke, M.; Steinemann, D.; Gross, M. (2005): Efficient animation of point-sampled thin shells. In *Computer Graphics Forum*, volume vol. 24, no. 3,, pp. 667–676.

Wu, X.; Shen, S.; Tao, W. (2007): Meshless local Petrov-Galerkin collocation method for two-dimensional heat conduction problems. *CMES-COMPUTER MODELING IN ENGINEERING & SCIENCES*, vol. 22, pp. 65–76.

Yuan, W.; Chen, P.; Liu, K. (2007): A new quasi-unsymmetric sparse linear systems solver for meshless local Petrov-Galerkin method (MLPG). *CMES-COMPUTER MODELING IN ENGINEERING & SCIENCES*, vol. 17, no. 2, pp. 115–134.

Zhang, Y.; Chen, L. (2008): A simplified meshless method for dynamic crack growth. *CMES-COMPUTER MODELING IN ENGINEERING & SCIENCES*, vol. 31, pp. 189–200.